

## Electric-field domains in semiconductor superlattices: Resonant and nonresonant tunneling

S.H. Kwok

*The Harrison M. Randall Laboratory of Physics, The University of Michigan, Ann Arbor, Michigan 48109-1120  
and Paul-Drude-Institut für Festkörperelektronik, Hausvogteiplatz 5-7, D-10117 Berlin, Germany*

R. Merlin

*The Harrison M. Randall Laboratory of Physics, The University of Michigan, Ann Arbor, Michigan 48109-1120*

H.T. Grahn and K. Ploog

*Paul-Drude-Institut für Festkörperelektronik, Hausvogteiplatz 5-7, D-10117 Berlin, Germany*

(Received 15 April 1994)

Photoluminescence experiments detecting the occupation of higher subbands in GaAs-Al<sub>x</sub>Ga<sub>1-x</sub>As superlattices are used to determine the field strengths of electric-field domains. While the magnitude of the electric field in the low-field domain corresponds to resonant alignment of subbands in adjacent wells, the field strength in the high-field domain is below the value corresponding to the resonant field. These results are interpreted in terms of a simple model based on current conservation.

The formation of electric-field domains in semiconductor superlattices is a consequence of negative differential resistance originating from resonant tunneling between different subbands in neighboring wells. The observation by Esaki and Chang<sup>1</sup> showed an oscillatory behavior of the conductance in *n*-doped GaAs-AlAs superlattices. More recently it was demonstrated that domain formation leads to extremely sharp jumps in the *I-V* characteristics with an average separation correlated with the subband spacing.<sup>2</sup> Domain formation in semiconductor superlattices has been observed in a variety of material systems,<sup>3-15</sup> but treated theoretically only by a small number of authors.<sup>11,16,17</sup> The field distribution in a weakly coupled superlattice containing a relatively large carrier density is not uniform. Instead, the field profile shows two regions referred to as domains where the field is given by the subband spacings of the individual quantum wells, i.e.,  $F_j = (E_j - E_1)/(de)$ , where  $E_j$  is the energy of the *j*th subband and  $d$  is the superlattice period. Photoluminescence (PL) experiments provide a direct proof of the existence of two regions with well-defined field strengths under domain formation.<sup>7,11,12</sup> Due to the different field strengths two clearly separated PL peaks are observed. The difference in peak energies originates from the quantum confined Stark effect (QCSE).<sup>18</sup>

In this paper we focus on a hitherto unrecognized aspect of the field distribution under domain formation. Because the field associated with the resonant coupling between  $e_1$  and  $e_j$  increases with increasing *j*, one expects that the larger the index *j*, the larger the resonant tunneling current. Due to current conservation, the magnitude of the field in high-field domains should be below the value corresponding to perfect subband alignment. This is to account for the fact that the largest possible current is always smaller in the low-field domain. In this paper we report on excited subband PL and intersubband Raman scattering experiments which demonstrate that the low-field domain is resonantly coupled, while the high-field domain is *nonresonantly* coupled with a field strength below the resonance value.

The samples were grown by molecular beam epitaxy on (100) *n*<sup>+</sup>-doped GaAs substrates. Sample *A* (*B*) consists of 100 (40) periods of 13.1 nm (9.0 nm) GaAs and 7.9 nm Al<sub>0.35</sub>Ga<sub>0.65</sub>As (4.0 nm AlAs) layers. Heavily doped *p*-type layers were deposited on the top of both superlattices to form *p-i-n* structures. The superlattices are not intentionally doped and the built-in voltage ( $V_0$ ) is 1.5 V. Sample *C* is a *n*<sup>+</sup>-*n*-*n*<sup>+</sup> superlattice with the same number of periods and well and barrier width as sample *B*. The central 5.0 nm of each well are doped at  $n = 3 \times 10^{17} \text{ cm}^{-3}$  with Si donors. The devices were processed into mesas of areas between 0.01 and 0.16 mm<sup>2</sup>. Ohmic Cr/Au and AuGe/Ni contacts are deposited on top and bottom. There is no evidence of domain formation in the dark *I-V* characteristic for the *p-i-n* structures. Due to heavy doping, domains already exist in sample *C* without photoexcitation. Raman measurements were performed using an Ar<sup>+</sup>-laser-pumped DCM dye laser tuned to  $\lambda = 638.2 \text{ nm}$ . This energy was chosen in order to resonantly excite the superlattice critical point derived from the  $E_0 + \Delta_0$  gap of GaAs. The PL spectra were obtained using the 676.4 nm of a Kr<sup>+</sup> laser. The measurements were performed at 4 K. In the undoped samples the domains were created by continuous photoexcitation (power  $\sim 10$ –50 mW). The current in the doped sample exhibited only a small change due to photoexcitation.

The field strength associated with the  $e_1 \rightarrow e_2$  resonance was measured using Raman scattering. Figure 1 shows the intersubband spectrum of sample *A* at  $-5 \text{ V}$ , where the negative sign denotes reverse bias. The energetic position of this peak remains constant between  $+1.5$  and  $-7 \text{ V}$ .<sup>13</sup> No significant shift is observed between the charge density  $z(x', x')\bar{z}$  and spin density  $z(x', y')\bar{z}$  peak positions.<sup>19</sup>  $x'$ ,  $y'$ , and  $z$  denote the [110], [110] and [001] directions, respectively. At larger electric fields the Raman peak shifts to higher energy since the subband separation increases with increasing electric field due to QCSE.<sup>20</sup> The experimentally determined separation between  $e_1$  and  $e_2$  is  $59.5 \pm 2.5 \text{ meV}$  between 1.5 and  $-7 \text{ V}$ . This value is slightly smaller than the

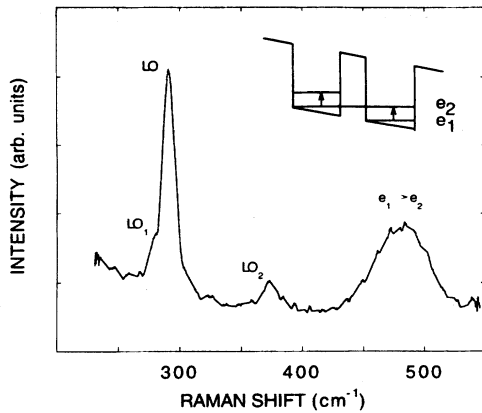


FIG. 1. Charge-density-excitation spectra of sample *A* at  $-5$  V. The feature labeled LO is the confined longitudinal-optical phonon of GaAs. LO<sub>1</sub> and LO<sub>2</sub> peaks are longitudinal-optical modes of the barrier layers, i.e., the GaAs-like and AlAs-like mode. The intersubband transition peak is labeled  $e_1 \rightarrow e_2$ . The inset shows a schematic energy diagram of the superlattice under  $e_1 \rightarrow e_2$  resonant tunneling condition.

calculated value (64 meV) based on growth parameters. Using Raman data the applied voltage for resonant coupling between  $e_1$  and  $e_2$  through the whole superlattice is  $-4.6 \pm 0.25$  V. Similar measurements have been performed on the other two samples (*B* and *C*) with a subband spacing of 137 meV.<sup>21</sup>

Recently, photoluminescence and electroluminescence experiments directly showed the occupation of higher subbands by resonant tunneling.<sup>22–25</sup> Thus the PL from higher subbands is extremely sensitive to the degree of level alignment between adjacent wells. Although the intensity of this higher subband PL is usually several orders of magnitude smaller than the band-gap PL, the higher lying peaks can be readily detected in weakly coupled superlattices. In Fig. 2 we com-

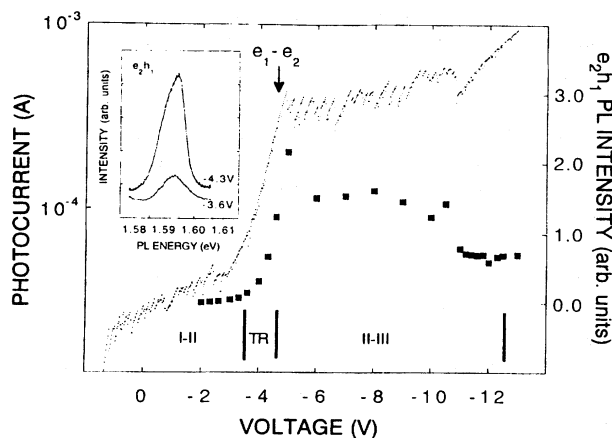


FIG. 2. Comparison between  $e_2h_1$  PL intensity (squares) and photocurrent (dots) for sample *A*. The arrow indicates the voltage corresponding to the  $e_1 \rightarrow e_2$  resonant alignment as determined by Raman scattering. Vertical solid lines separate different domain regimes (e.g., I-II indicate coexistence of domains I and II, TR stands for transition region). The inset illustrates the  $e_2h_1$  intensity enhancement at  $-3.5$  V.

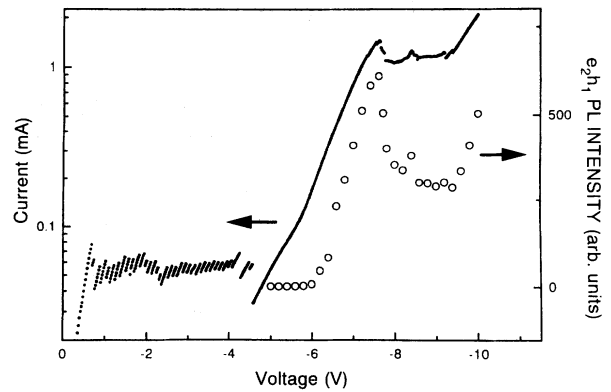


FIG. 3. Comparison between  $e_2h_1$  PL intensity (circles) and total current (small dots) for sample *C*.

pare the voltage dependence of the  $e_2h_1$  PL intensity with that of the photocurrent for sample *A*.  $e_ih_j$  denotes the transition of an electron in the  $i$ th subband and a heavy hole in the  $j$ th subband. Vertical lines divide the diagram into voltage regions I-II and II-III. Here, I-II (II-III) labels the region of coexistence of domains I and II (II and III).

In the transition region between regimes I-II and II-III ( $-3.5$  to  $-4.6$  V), there is a range where the current and the  $e_2h_1$  PL intensity rise abruptly. Previous studies provided no satisfactory explanation for such a behavior. The most striking point of the  $e_2h_1$  PL data is that the PL line indicating resonant alignment between  $e_1$  and  $e_2$  only emerges for voltages beyond  $-3.5$  V and reaches its maximum at  $-4.6$  V. This observation clearly demonstrates that the high-field domain exhibits a field strength below  $F_2 = (E_2 - E_1)/(ed)$ . Only when the high-field domain (II) becomes a low-field domain, i.e., beyond  $-4.6$  V, its field strength corresponds to the resonance field strength. The inset of Fig. 2 illustrates the sudden appearance of the  $e_2h_1$  PL peak. Notice that the  $e_3h_1$  PL line emerges only beyond  $-12.5$  V. This again demonstrates that the high-field domain (III) in this regime is such that the magnitude of the field is below  $F_3$ .

Figure 3 compares the  $e_2h_1$  PL intensity and the total current in the doped sample. Again no  $e_2h_1$  PL signal is observed in the first plateau region where domains I and II coexist. The  $e_2h_1$  line emerges only beyond  $-5$  V, and its intensity increases proportional to the total current. This clearly indicates that also in the doped sample, where only electrons contribute to the current, the high-field domain (II) exhibits a field strength below the resonant field  $F_2$ . It is only at the onset of the next plateau that the field strength reaches  $F_2$ . In the transition region (TR), the field is uniform over the whole superlattice. Similar results were obtained for the undoped sample *B*.

Before we give a detailed account of these observations, it is instructive to understand the qualitative relationship between the current and the  $e_jh_1$  ( $j > 1$ ) PL intensity in the vicinity of a tunneling resonance. Under steady state conditions, the ratio between the electron concentration in the  $j$ th ( $n_j$ ) and the first subband ( $n_1$ ) at the resonance field  $F_j$  is given by

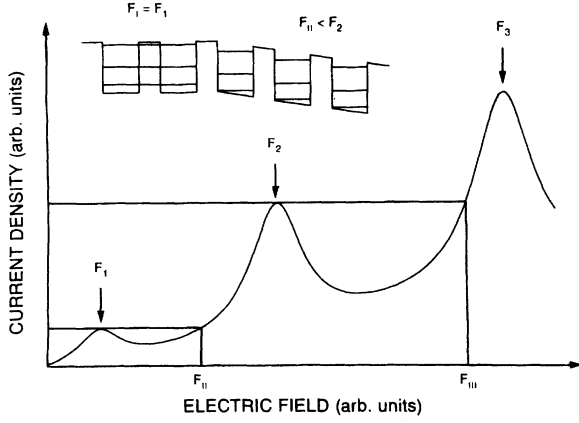


FIG. 4. Current-field characteristics of an undoped superlattice. The three peaks at  $F_1$ ,  $F_2$ , and  $F_3$  are due to  $e_1 \rightarrow e_1$ ,  $e_1 \rightarrow e_2$ , and  $e_1 \rightarrow e_3$  resonant alignment, respectively. The current is conserved only when  $F_{II}$  is smaller than  $F_2$ . Inset: Schematic diagram showing coexistence of domains I and II. Current conservation requires that  $F_{II} < F_2$ .

$$\frac{n_j}{n_1} = \frac{\tau_{j1}}{\tau_{tran}}, \quad (1)$$

where  $\tau_{j1}$  is the intersubband scattering time from the  $j$ th to the first subband and  $\tau_{tran}$  is the well-to-well transit time. In Eq. (1) electron-hole recombination is not taken into account. Furthermore, tunneling out of the higher subbands into adjacent wells is neglected and carriers are assumed to be present mainly in the first subband. We know that there is a strong correlation between  $n_2$  and the current when the field strength in domain II ( $F_{II}$ ) becomes  $F_2$ . The current density  $J$  is approximately proportional to the two-dimensional carrier density in the first subband of each well divided by the transit time between adjacent wells. Together with Eq. (1) it follows that

$$J \approx \frac{n_1}{\tau_{tran}} = \frac{n_2}{\tau_{21}}. \quad (2)$$

$\tau_{tran}$  becomes very small under resonant tunneling conditions. Since  $\tau_{21}$  does not vary very much with the field strength,<sup>26</sup> the current density is proportional to  $n_2$ . When the voltage drop per well approaches the condition for resonant tunneling, i.e., when it is equal to the subband spacing divided by the electron charge, the current density  $J$  as well as the  $e_2h_1$  PL intensity rise abruptly due to the reduction of  $\tau_{tran}$ .

To account for our observations, a simple model is discussed which includes the finite width and the different peak currents of the resonances. Figure 4 illustrates a schematic diagram of typical current-field characteristics of an undoped superlattice. The three peaks at  $F_1$ ,  $F_2$ , and  $F_3$  are due to  $e_1 \rightarrow e_1$ ,  $e_1 \rightarrow e_2$ , and  $e_1 \rightarrow e_3$  resonant alignments of subbands, respectively. The condition determining the domain field strength is the conservation of current through the superlattice. In a very simple theoretical treatment of domain formation using infinitesimally sharp peaks for the resonances the field strengths of the domains are given by the resonance fields  $F_j$ .<sup>11</sup> When the broadening of the reso-

nances and different peak heights are included, the actual field of the domains will differ from the resonance field. The first instability occurs when the field exceeds  $F_1$ . Here, the sample breaks into domains I and II (see inset of Fig. 4). Since the current through the sample is conserved,  $F_{II}$  has to be smaller than the resonant field  $F_2$ . This conclusion is supported by theoretical calculations of the field distribution in the superlattice under domain formation<sup>27</sup> using a microscopic model.<sup>28</sup> This is consistent with the fact that we do not observe a  $e_2h_1$  PL signal in the I-II regime. At the end of the first oscillatory region in the  $I$ - $V$  characteristics the entire superlattice is in a single domain II for which the field strength is smaller than  $F_2$ . In the first transition region, the field is uniform and its value increases to  $F_2$  as the applied voltage increases. For the undoped samples this interpretation is also consistent with our earlier estimate using the Raman scattering results. However, in the doped sample the onset voltage of the second plateau is considerably larger than the value predicted by the subband spacing, which is probably due to an additional voltage drop in the contact regions. As the voltage drop across the superlattice reaches the condition of resonant tunneling, the  $e_2h_1$  PL intensity and the photocurrent rise abruptly in the first transition region according to Eq. (2).

For the second plateau we consider sample A. Between  $-4.6$  and  $-12.5$  V, this sample is in the second instability region (cf. Fig. 4) in which domains II and III coexist. A single PL line is observed in the  $e_2h_1$  spectral region compared to the  $e_1h_1$  doublet. Its energetic position does not change much with increasing field. This observation reflects the much larger  $e_2$  population in domain II arising from  $e_1 \rightarrow e_2$  resonant tunneling, when domain II becomes a low-field domain. The decrease in  $e_2h_1$  PL intensity with increasing voltage in the II-III region results from a reduction of the spatial extent of domain II. The absence of  $e_3h_1$  PL in the second current plateau (between  $-4.6$  and  $-12.5$  V) indicates again that the field strength of the high-field domain (III) is smaller than  $F_3$  in the domain II-III regime. The subband alignment in domain III is below the  $e_1 \rightarrow e_3$  resonance so that the current is conserved. At  $-12.5$  V the field is uniform throughout the whole superlattice. The  $e_3h_1$  PL intensity rises together with the current beyond  $-12.5$  V, implying that the field strength in domain III increases to a value equal to  $F_3$  during the second transition ( $-12.5$  to  $-14$  V). This again demonstrates that in the domain II-III regime the low-field domain is resonantly coupled, while the field strength in the high-field domain is below the resonance field  $F_3$ .

In summary, the field strengths of electric-field domains in semiconductor superlattices have been determined directly by photoluminescence and Raman scattering experiments. Using the PL from higher subbands it is clearly shown that the magnitude of the electric field in the low-field domains corresponds to the tunneling resonance field, while the field in the high-field domain is below the corresponding resonant field. The PL signal from higher subbands appears only when the next transition region between the plateaus of the  $I$ - $V$  characteristics is reached. The resulting field values are a direct consequence of current conservation.

We would like to thank E. Liarokapis for his scientific support during the initial stages of this work, S. Murugkar and A. Wacker for helpful discussions, and M. Ramsteiner for experimental support and a critical reading of the manu-

script. This work was supported in part by the U.S. Army Research Office under Contract No. DAAL-03-92-G-0233 and the National Science Foundation through the Center for Ultrafast Optical Science under STC No. PHY 8920108.

- 
- <sup>1</sup>L. Esaki and L.L. Chang, *Phys. Rev. Lett.* **33**, 495 (1974).
  - <sup>2</sup>H.T. Grahn, R.J. Haug, W. Müller, and K. Ploog, *Phys. Rev. Lett.* **67**, 1618 (1991).
  - <sup>3</sup>Y. Kawamura, K. Wakita, H. Asaki, and K. Kurumada, *Jpn. J. Appl. Phys.* **25**, L928 (1986).
  - <sup>4</sup>K.K. Choi, B.F. Levine, R.J. Malik, J. Walker, and C.G. Bethea, *Phys. Rev. B* **35**, 4172 (1987).
  - <sup>5</sup>K.K. Choi, B.F. Levine, N. Jarosik, J. Walker, and R. Malik, *Phys. Rev. B* **38**, 12 362 (1988).
  - <sup>6</sup>R.E. Cavicchi, D.V. Lang, D. Gershoni, A.M. Sergent, H. Temkin, and M.B. Panish, *Phys. Rev. B* **38**, 13 474 (1988).
  - <sup>7</sup>H.T. Grahn, H. Schneider, and K. v. Klitzing, *Appl. Phys. Lett.* **54**, 1757 (1989).
  - <sup>8</sup>E.S. Snow, S.W. Kirchoefer, and O.J. Glembocki, *Appl. Phys. Lett.* **54**, 2023 (1989).
  - <sup>9</sup>M. Helm, P. England, E. Colas, F. DeRosa, and S.J. Allen, Jr., *Phys. Rev. Lett.* **63**, 74 (1989).
  - <sup>10</sup>T.H.H. Vuong, D.C. Tsui, and W.T. Tsang, *J. Appl. Phys.* **66**, 3688 (1989).
  - <sup>11</sup>H.T. Grahn, H. Schneider, and K. v. Klitzing, *Phys. Rev. B* **41**, 2890 (1990).
  - <sup>12</sup>M. Helm, J.E. Golub, and E. Colas, *Appl. Phys. Lett.* **56**, 1356 (1990).
  - <sup>13</sup>S.H. Kwok, E. Liarokapis, R. Merlin, and K. Ploog, in *Light Scattering in Semiconductor Structures and Superlattices*, edited by D.J. Lockwood and J.F. Young (Plenum, New York, 1991), p. 491.
  - <sup>14</sup>H.T. Grahn, W. Müller, K. v. Klitzing, and K. Ploog, *Surf. Sci.* **267**, 579 (1992).
  - <sup>15</sup>I. Gravé, A. Shakouri, N. Kuze, and A. Yariv, *Appl. Phys. Lett.* **60**, 2362 (1992).
  - <sup>16</sup>B. Laikhtman, *Phys. Rev. B* **44**, 11 260 (1991).
  - <sup>17</sup>A.N. Korotkov, D.V. Averin, and K.K. Likarev, *Appl. Phys. Lett.* **62**, 3282 (1993).
  - <sup>18</sup>D.A.B. Miller, D.S. Chemla, T.C. Damen, A.C. Gossard, W. Wiegmann, T.H. Wood, and C.A. Burrus, *Phys. Rev. Lett.* **53**, 2173 (1984).
  - <sup>19</sup>A. Pinczuk and G. Abstreiter, in *Light Scattering in Solids V*, edited by M. Cardona and G. Güntherodt, *Topics in Applied Physics Vol. 66* (Springer, Berlin, 1989), p. 153.
  - <sup>20</sup>K. Bajema, R. Merlin, F.-Y. Juang, S.-C. Hong, J. Singh, and P.K. Bhattacharya, *Phys. Rev. B* **36**, 1300 (1987).
  - <sup>21</sup>S. Murugkar, S.H. Kwok, G. Ambrazevičius, H.T. Grahn, K. Ploog, and R. Merlin, *Phys. Rev. B* (to be published).
  - <sup>22</sup>H.T. Grahn, H. Schneider, W.W. Rühle, K. v. Klitzing, and K. Ploog, *Phys. Rev. Lett.* **64**, 2426 (1990).
  - <sup>23</sup>H.T. Grahn, W.W. Rühle, K. v. Klitzing, and K. Ploog, *Semicond. Sci. Technol.* **7**, 3409 (1992).
  - <sup>24</sup>D. Bertram, H. Lage, H.T. Grahn, and K. Ploog, *Appl. Phys. Lett.* **64**, 1012 (1994).
  - <sup>25</sup>S.H. Kwok, H.T. Grahn, K. Ploog, and R. Merlin, *Phys. Rev. Lett.* **69**, 973 (1992).
  - <sup>26</sup>R. Ferreira and G. Bastard, *Phys. Rev. B* **40**, 1074 (1989).
  - <sup>27</sup>F. Prengel, A. Wacker, and E. Schöll (private communication).
  - <sup>28</sup>F. Prengel, A. Wacker and E. Schöll, *Phys. Rev. B* (to be published).